AD-765 764

IMPROVED MODE PROPERTIES OF UNSTABLE
RESONATORS WITH TAPERED REFLECTIVITY
MIRRORS AND SHAPED APERTURES

G. L. McAllister, et al

Northrop Research and Technology Center

Prepared for:

Advanced Research Projects Agency
Office of Naval Research

August 1973

AD-765764

NRTC 73-33R

IMPROVED MODE PROPERTIES OF UNSTABLE RESONATORS WITH TAPERED REFLECTIVITY MIRRORS AND SHAPED APERTURES

DDC
AUG 30 1973
F

August 1973

Prepared by

G. L. McAllister, W. H. Steier, and W. B. Lacina

Northrop Research and Technology Center
3401 West Broadway
Hawthorne, California 90250

NOTICE

The views and conclusions contained in this document
are those of the author and should not be interpreted
as necessarily representing the official policies, either
expressed or implied, of the Advanced Research Projects
Agency or the U.S. Government.

REPORT DOCUMENTATION PAGE		READ INSTRUCTIONS BEFORE COMPLETING FORM
1. REPORT NUMBER NRTC 73-33R	2. GOVT ACCESSION NO.	3. RECIPIENT'S CATALOG NUMBER
4. TITLE *(and Subtitle)* Improved Mode Properties of Unstable Resonators with Tapered Reflectivity Mirrors and Shaped Apertures		5. TYPE OF REPORT & PERIOD COVERED Technical Report
		6. PERFORMING ORG. REPORT NUMBER
7. AUTHOR(s) G. L. McAllister, W. H. Steier, W. B. Lacina		8. CONTRACT OR GRANT NUMBER(s) N00014-72-C-0043
9. PERFORMING ORGANIZATION NAME AND ADDRESS Northrop Research and Technology Center 3401 West Broadway Hawthorne, California 90250		10. PROGRAM ELEMENT, PROJECT, TASK AREA & WORK UNIT NUMBERS ARPA Order No. 1806
11. CONTROLLING OFFICE NAME AND ADDRESS Advanced Research Projects Agency 1400 Wilson Blvd. Arlington, Virginia 22209		12. REPORT DATE August 1973
		13. NUMBER OF PAGES ~~42~~ 44
14. MONITORING AGENCY NAME & ADDRESS*(If different from Controlling Office)* Office of Naval Research Department of the Navy Arlington, Virginia 22217		15. SECURITY CLASS. *(of this report)* UNCLASSIFIED
		15a. DECLASSIFICATION DOWNGRADING SCHEDULE

16. DISTRIBUTION STATEMENT *(of this Report)*

None.

17. DISTRIBUTION STATEMENT *(of the abstract entered in Block 20, If different from Report)*

None.

18. SUPPLEMENTARY NOTES

None.

19. KEY WORDS *(Continue on reverse side if necessary and identify by block number)*

Unstable Resonators
Mirror Edge Effects
Aperture Shaping

20. ABSTRACT *(Continue on reverse side if necessary and identify by block number)*

The use of tapered reflectivity mirrors and shaped apertures in unstable resonators is shown to be an effective method for improving the mode properties. Mode intensity and phase profiles are smoothed and the mode discrimination ratio is increased. Results are presented illustrating the importance of diffracted waves from sharp mirror edges in determining these mode properties. A simple expression for estimating the diffractive contribution is given and is used to determine optimum mirror designs. Shaped mirrors

DD _{1 JAN 73} FORM 1473   EDITION OF 1 NOV 65 IS OBSOLETE

1a

20. and mirrors having amplitude and phase reflectivity tapers are studied. The concept of equivalent Fresnel zones is used to gain physical insight into the mode properties.

iii

TABLE OF CONTENTS

ABSTRACT

The use of tapered reflectivity mirrors and shaped apertures in unstable resonators is shown to be an effective method for improving the mode properties. Mode intensity and phase profiles are smoothed and the mode discrimination ratio is increased. Results are presented illustrating the importance of diffracted waves from sharp mirror edges in determining these mode properties. A simple expression for estimating the diffractive contribution is given and is used to determine optimum mirror designs. Shaped mirrors and mirrors having amplitude and phase reflectivity tapers are studied. The concept of equivalent Fresnel zones is used to gain physical insight into the mode properties.

I. INTRODUCTION

Numerous theoretical studies of unstable resonators[1] with mirrors having sharp edges have shown characteristics which are quite different from those of stable resonators. The unstable resonator mode shapes and losses are sensitively dependent upon the mirror radii and curvatures in contrast to the stable resonator modes which change only slowly with the mirror parameters.[2] The manner in which the modes vary with the parameter N_{eq} (the equivalent Fresnel number defined by Siegman and Arrathoon[3]) is particularly interesting. Siegman and Miller[4] have shown that the mode losses for cylindrical unstable resonators not only interleave but have minima and crossover points which are periodic with, respectively, half integer and integer values of this parameter N_{eq}. Anan'ev[5] has pointed out that, for unstable resonators, the diffracted wave or "edge" wave resulting from the sharp edge of the mirror will have a dominant effect on the mode properties and accounts for the periodic behavior. In addition, he has suggested that eliminating the sharp edge condition will result in modes more like the geometrical optics values, improving both the mode shapes and discrimination ratios.

In this paper we explore in more detail the effects of the aperture edge and illustrate the advantages of tapering the mirror edges, both in amplitude and phase. A theory is developed which helps in the design of tapered mirror resonators and which predicts the effects of aperture shaping without recourse to extensive computer calculations. The parameter N_{eq} comes in naturally in this theory and its physical significance becomes more apparent. It will be shown by comparisons with detailed computer calculations for several examples that the present theory successfully predicts the significant features of the resonator modes. Finally, the application of these techniques to the design of practical

1

resonators shall be discussed, particularly for resonators with large Fresnel numbers such as those presently used for high power gas lasers.

It is found that the degree of mode improvement effected by edge tapering is dependent upon the exact nature of the taper.[6] As an illustration, consider the fundamental modes for three symmetric unstable resonators (N_{eq} = 2.8, M = 2.0) having mirror reflectivities which vary with radius as shown in Figure 1. The computer calculated normalized intensity profiles for these three cases are shown in Figure 2. Although the linear and parabolic taper functions appear very similar, the modes are quite different, with the parabolic taper producing a much smoother mode. It is usually found, as is demonstrated by the two tapers here, that any taper, even though it is not optimized, will improve the mode over the sharp edge case. The phase profiles (normalized to the geometrical optics values) are shown in Figure 3 and are even more striking. The sharp edge case shows a variation of almost $\lambda/4$ (unacceptable for diffraction-limited operation) whereas the parabolic taper has essentially no deviation beyond the center 10%. These results are consistent with the theory, which predicts that the linear taper should be an improvement over the sharp edge and that a parabolic taper over the outer 20% should be nearly optimum and result in a uniform mode similar to the geometrical optics solution.

II. THEORY

The concept of an edge wave, i.e. a diffracted wave which emanates from an aperture edge, can be obtained from standard scalar diffraction theory as described by Born and Wolf.[7] This concept is discussed in more detail below but, in brief, the edge wave formalism is obtained by expressing the field amplitude resulting from an illuminated aperture as the sum of a geometrical optics term plus a diffraction term, the latter of which is expressed as a line integral around the aperture boundary. The diffracted wave is emitted in all directions but, as Anan'ev has pointed out, only that
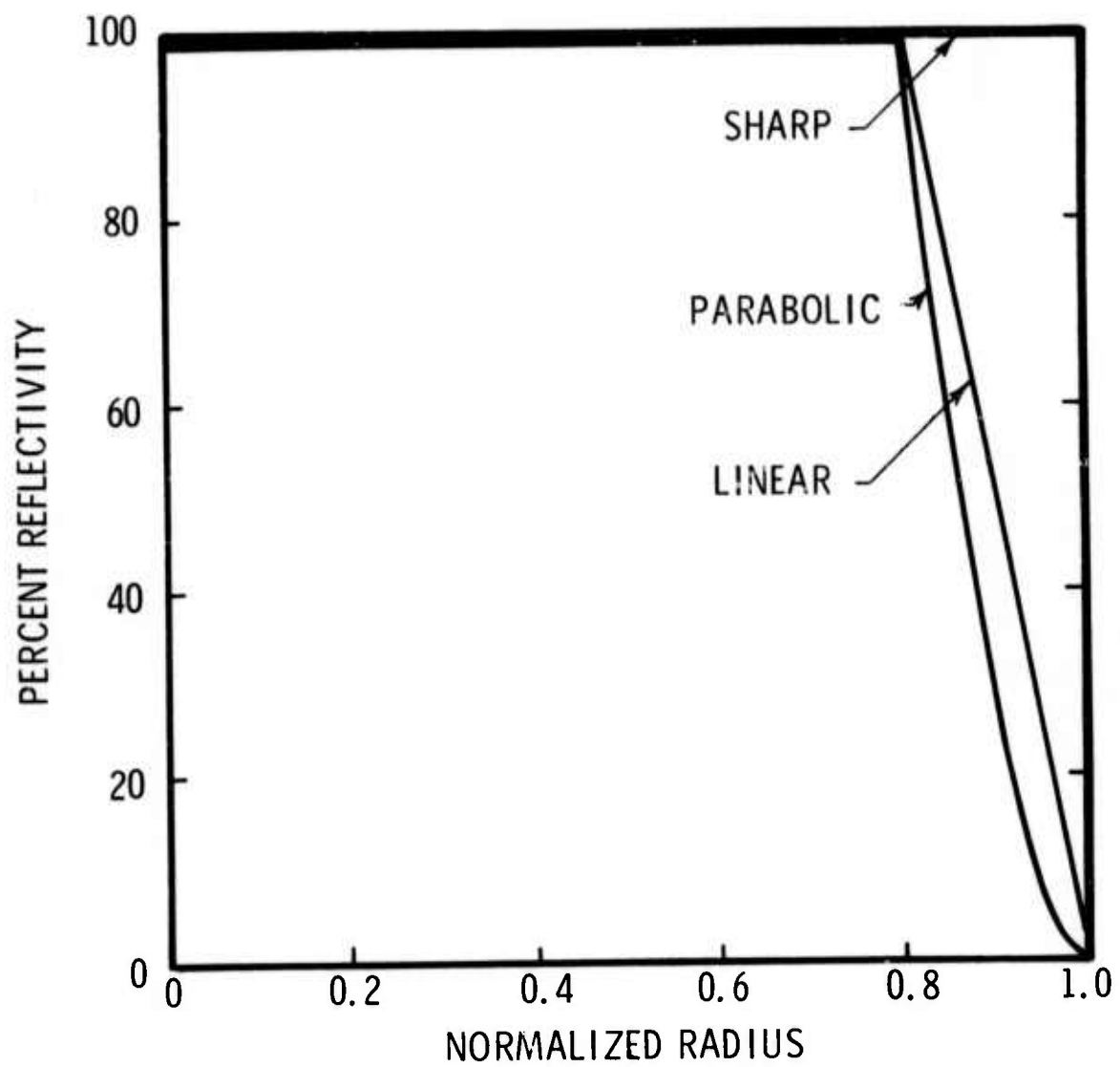
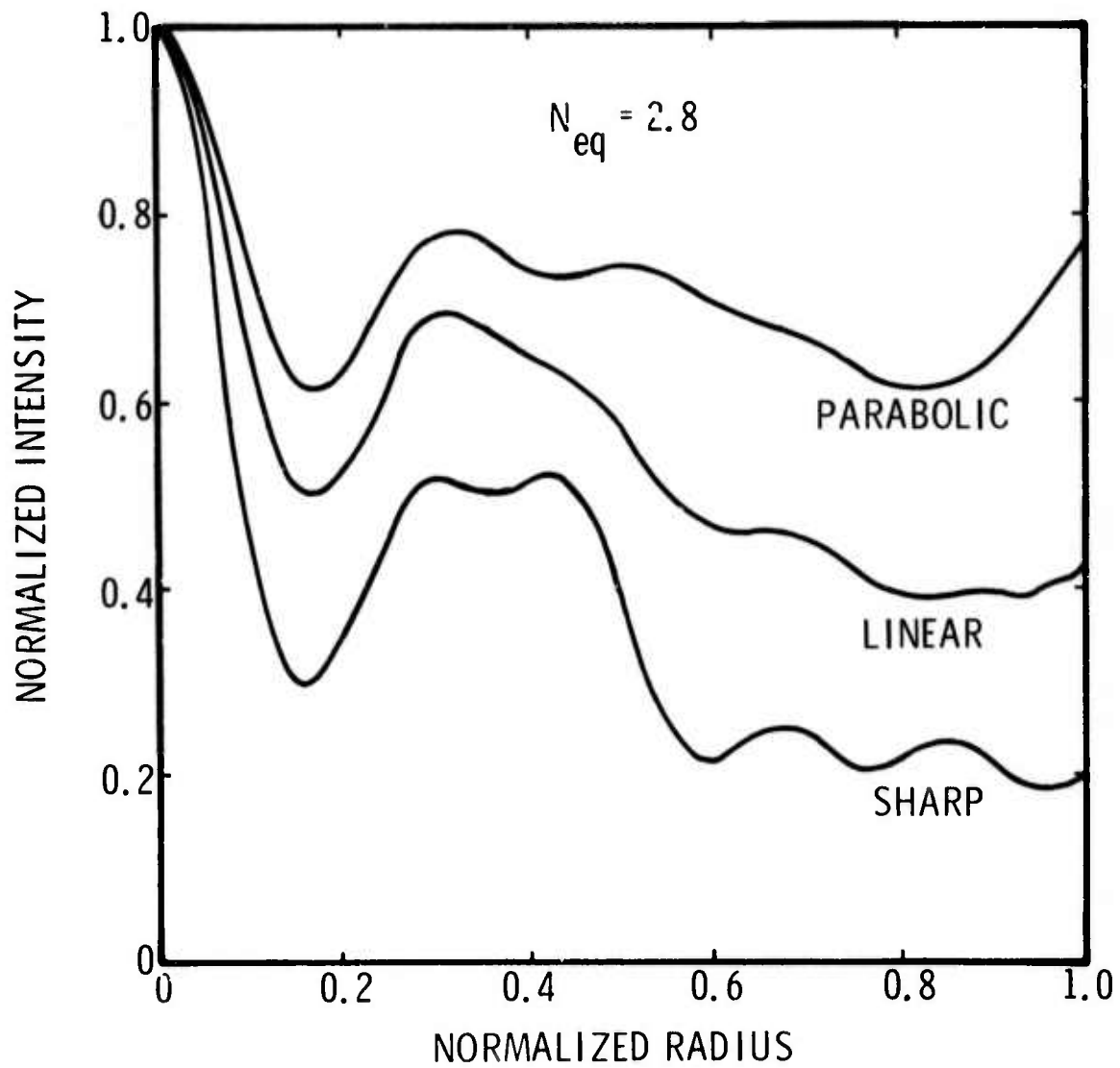Figure 1.   Amplitude reflectivity vs normalized mirror radius.

Figure 2. Normalized mode intensity profiles for symmetric resonators with tapered reflectivity mirrors. $N_{eq} = 2.8$
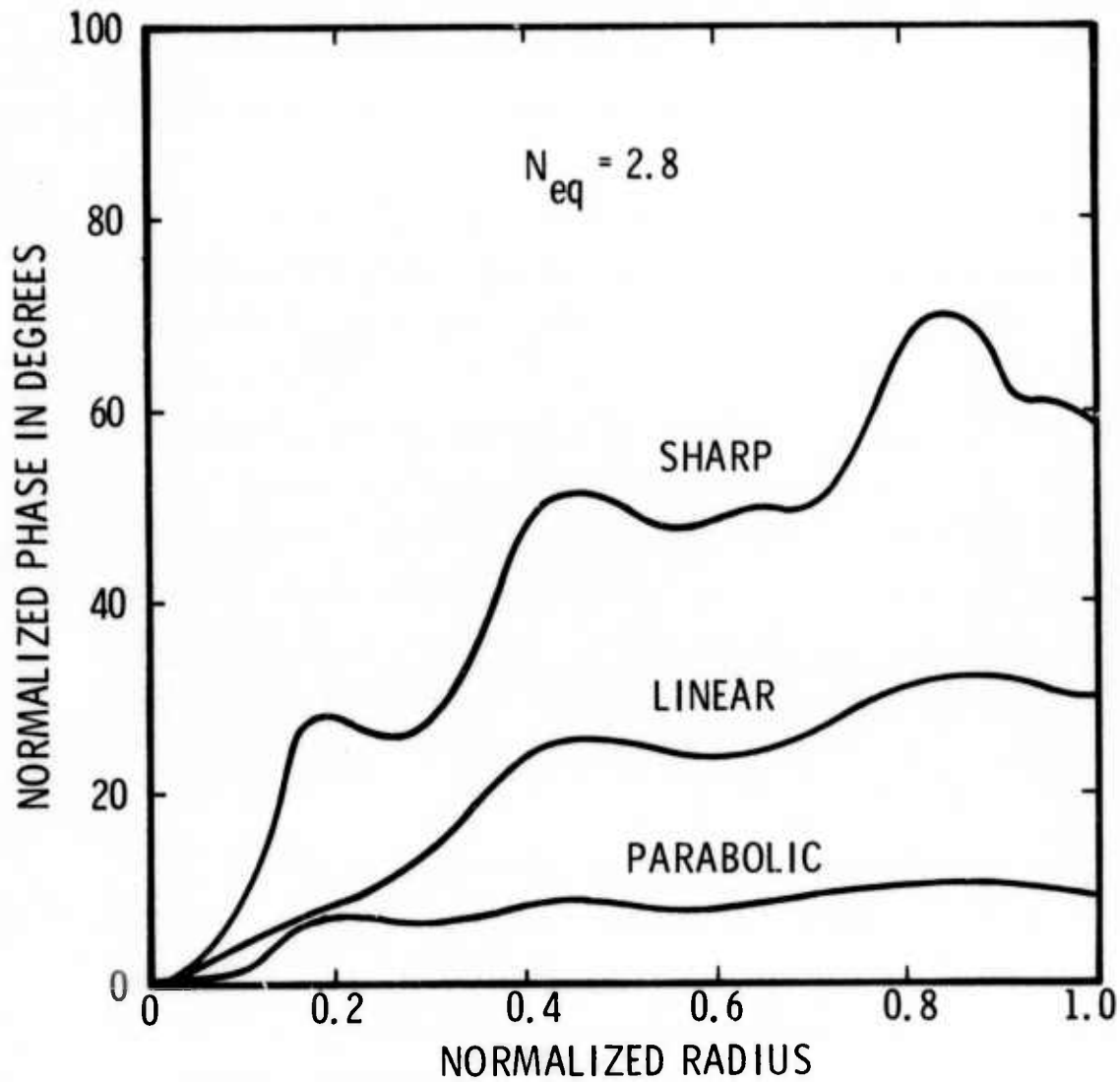
Figure 3. Normalized mode phase profiles for symmetric
unstable resonators with tapered reflectivity
mirrors. $N_{eq} = 2.8$

5

part of the edge wave which is directed back into the cavity such that it is trapped along the resonator axis should be important in determining the properties of the modes. This is illustrated for a symmetric unstable resonator in Figure 4. The solid lines represent the geometrical rays of the resonator mode which are incident on the sharp edge of the mirror and the dashed lines represent rays of the resulting edge wave. It is clear that the diffracted rays which are scattered in a direction exactly opposite to that of the ray incident on the mirror edge will, in the geometrical optics picture, be trapped along the resonator axis whereas the other diffracted waves will be deflected out of the cavity after a few reflections. These rays which are trapped in the geometrical optics picture will of course diverge due to diffraction and thus act in part as the source for the mode.

The phase shift between two trapped rays originating from different radii at the aperture is the same, after many round trips, as the phase difference between the two rays if they are extended directly to the virtual focus (Point P_0 in Figure 4). Thus a semi-quantitative measure of the diffractive contribution to the mode can be obtained by computing the edge diffracted field amplitude at the virtual focus resulting from the mirror (or aperture) illumination.

It is obvious from symmetry that the rays from the sharp edge of a cylindrical mirror will all arrive at the virtual focus in phase. This produces a large diffractive contribution, resulting in modes with large amplitude variations across the radius, large phase deviations from the geometrical optics value and mode losses which vary rapidly with the resonator parameters. It is also clear that altering the shape of the aperture or tapering the edge such that it is no longer sharp can result in destructive interference at the focus, reducing the diffractive contribution to the modes. Anan'ev has suggested that these destructive interference effects can be introduced by smoothly rolling off the mirror edges, roughing
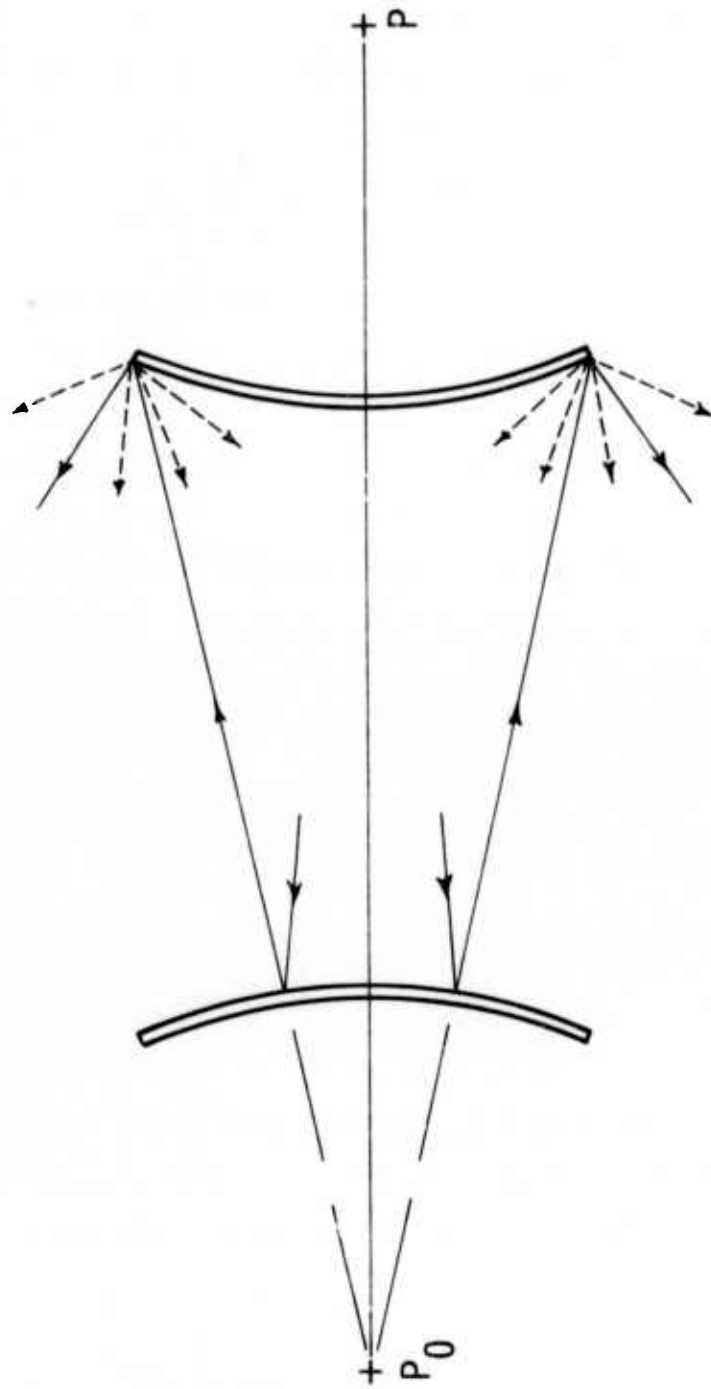
6

Figure 4.   Geometrical description of edge wave diffraction in a symmetrical unstable resonator.

the edges, misalignment, positioning the mirror off center, etc., over a zone of width $a/2N_{eq}$ where a is the mirror radius. We consider here the effects of amplitude tapering, introduced by varying the mirror reflectivity with radius; phase tapering, introduced by rolling off the mirror edges; and aperture shaping.

Mathematical formulation of edge wave effects can be obtained from the standard Kirchhoff approximations used in scalar diffraction theory, with the diffraction contribution expressed as a line integral around the aperture boundary. By superposition we can treat the variable transmission aperture (or the variable reflectivity mirror) as a sum of sharp edge apertures, each illuminated by a spherical wave, with amplitude and phase such that the sum equals the proper field amplitude at the aperture. If we consider, as shown in Figure 5, an aperture illuminated by a spherical wave $U_o \exp(ikr)/r$ emanating from the point P_o, then the field amplitude at a point P can be written as

$$U(P) = \frac{1}{4\pi} \iint_A U_o \left\{ \frac{\exp(ikr)}{r} \frac{\partial}{\partial n} \left[\frac{\exp(iks)}{s} \right] - \frac{\exp(iks)}{s} \frac{\partial}{\partial n} \left[\frac{\exp(ikr)}{r} \right] \right\} dS \qquad (1)$$

where r is the distance from P_o to a point in the aperture plane A, s is the distance from P to the same point in the aperture plane, $\partial/\partial n$ is the derivative along the inward normal to the surface and $k = 2\pi/\lambda$ is the wave number.

Following Born and Wolf,[7] Equation (1) can be written as the sum of a geometrical optics term and a diffractive term,

$$U(P) = U_G(P) + U_D(P), \qquad (2)$$

8

Figure 5. Coordinate system for calculation of the diffraction fields of an aperture.

where

$$U_G(P) = U_o \exp(ikR)/R \qquad (3)$$

and

$$U_D(P) = -\frac{1}{4\pi} \iint_B U_o \left\{ \frac{\exp(ikr)}{r} \frac{\partial}{\partial n} \left[\frac{\exp(iks)}{s} \right] \right.$$
$$\left. - \frac{\exp(iks)}{s} \frac{\partial}{\partial n} \left[\frac{\exp(ikr)}{r} \right] \right\} dS. \qquad (4)$$

In this equation, $\vec{R}$ is the vector from P_o to P, and B is that part of an infinite conical surface originating at P_o which subtends and lies to the right of the aperture boundary Γ. The surface integral that occurs in Equation (4) for U_D can be transformed into a line integral around the aperture boundary Γ using a Rubinowicz representation:

$$U_D(P) = \frac{1}{4\pi} \oint_\Gamma \left\{ \frac{\exp[ik(r_1+s_1)]}{r_1 s_1} \cdot \frac{\cos(\vec{n},\vec{s}_1) \sin(\vec{r}_1, \vec{d\ell})}{1+\cos(\vec{r}_1,\vec{s}_1)} \right\} d\ell, \qquad (5)$$

where $\vec{r}_1$ and $\vec{s}_1$ are vectors to a point on the aperture boundary from P_o and P, respectively, $\vec{d\ell}$ is a differential line element along the boundary, and $\vec{n}$ is a unit normal vector directed inward from the surface B. Equation (5) can be simplified considerably for cases where the source point P_o is directly behind the aperture and the angles θ and φ that $\vec{r}_1$ and $\vec{s}_1$ make with $\vec{R}$ (shown in Figure 5) are small, which is the case for aligned resonators with moderate Fresnel numbers. In that case, $\sin(\vec{r}_1, \vec{d\ell}) \approx 1$, $\cos(\vec{n}_1 \vec{s}_1) \approx -(\theta+\varphi)$ and

$$1 + \cos(\vec{s}_1, \vec{r}_1) \approx (\theta+\varphi)^2/2. \qquad (6)$$

10

These approximations will not introduce serious errors in Equation (3) since they do not occur in the phase term.

Substituting

$$\theta + \phi \approx \frac{\xi(r_1 + s_1)}{r_1 s_1} \quad , \tag{7}$$

where ξ is the distance between a point on the boundary and the intercept of the line $P_o P$ with the aperture A,

$$U_D(P) = \frac{-1}{2\pi} \oint_\Gamma \frac{U_o \exp[ik(r_1 + s_1)]}{\xi(r_1 + s_1)} \, d\ell \quad . \tag{8}$$

These results can be applied to a symmetric resonator, as shown in Figure 6. The philosophy of the present approach assumes that, to the lowest order of approximation, the modes of a resonator are described by the geometrical solution. Diffraction effects, calculated from Kirchoff theory with the assumption that apertures are illuminated by the zeroth order geometrical fields, then enter as a first order correction. Since the geometrical solution for a resonator with perfectly reflecting spherical mirrors is equivalent to two point sources of radiation placed at the virtual foci P_o and Γ, we assume that the left mirror in Figure 6 is illuminated by a uniform spherical wave emanating from the virtual focus P_o, and estimate the resulting diffraction effects at the opposite virtual focus P. In actuality, the mirror illumination is not uniform and the theory is only approximate in that sense. However, we will search for conditions where the diffractive contributions are minimum, which are also the conditions where the approximation of the uniform wave are most accurate.

The lengths shown in Figure 6 (given by Siegman) can be used to formulate Equation (8) in terms of the equivalent Fresnel number. At this point,
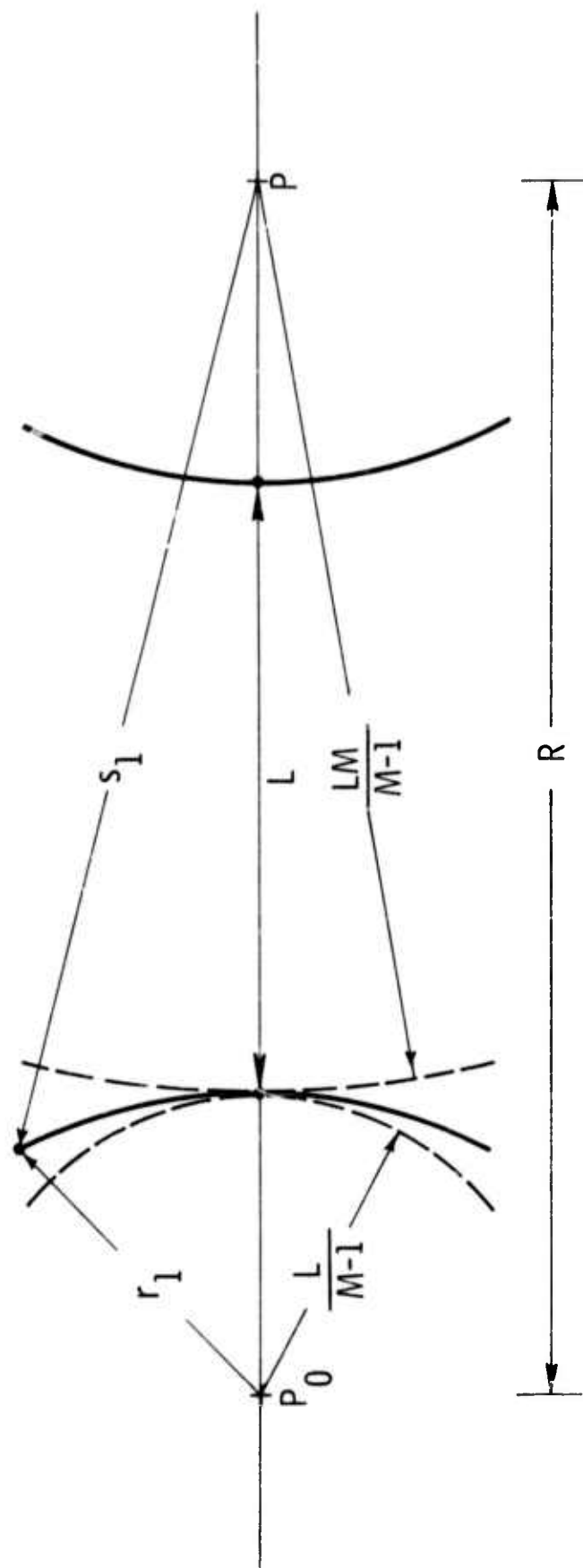
11

Figure 6. Coordinate system for calculating the edge diffraction in a symmetric unstable resonator.

a shape for the boundary has not been specified and N_{eq} is thus still a function of the radial coordinate ξ.

If the mirror size is small compared to $L/(M-1)$ and $LM/(M-1)$ then

$$r_1 + s_1 \approx R + \frac{\xi^2(M-1)}{2L} + \frac{\xi^2(M-1)}{2LM} \tag{9}$$

and

$$k(r_1 + s_1) = kR + \frac{\pi\xi^2}{L\lambda}(M-1/M) , \tag{10}$$

The equivalent Fresnel number at radius ξ is defined as

$$N_{eq}(\xi) = \frac{\pi\xi^2}{2L\lambda}(M-1/M)$$

hence

$$k(r_1 + s_1) = kR + 2\pi N_{eq}(\xi). \tag{11}$$

The diffraction contribution Equation (8) becomes, after approximating $(r_1 + r_2) \approx R$ in the demoninator,

$$U_D(P) = -\frac{\exp(ikR)}{2\pi R} \oint_\Gamma U_o \frac{\exp[i2\pi N_{eq}(\xi)]d\ell}{\xi} , \tag{12}$$

and, if the mirrors are circular with radius ξ, this becomes

$$U_D(P) = -\frac{\exp(ikR)}{R} U_o \exp[i2\pi N_{eq}(\xi)]. \tag{13}$$

13

Consider now a resonator with circular mirrors of radius a which have nonuniform reflectivities or which are not spherical. In this case, the equivalent aperture illumination must now be described by replacing the constant U_o by a complex function $U(\xi)$, where the amplitude and phase of $U(\xi)$ express variation in mirror reflectivity and deviation of reflected phase fronts from the geometrical phase fronts. Because of the assumed circular symmetry of the mirrors, $U(\xi)$ is a function of the radial coordinate only. The diffracted wave from this nonuniformly illuminated aperture can be expressed with the edge wave formalism of Equation (13) by a superposition of uniformly illuminated circular apertures of varying radii with different amplitudes and phases. If an aperture of radius ξ is illuminated by $(dU/d\xi)\,\Delta\xi$ [corresponding to U_o of Equation (13)], then the summation of the fields of all these apertures will be $U(\xi)$. The diffracted field at P from each of these apertures can be obtained from Equation (13), and when summed, give the total diffracted field at P due to the distribution $U(\xi)$:

$$U_D(P) = -\frac{\exp(ikR)}{R} \int_0^1 \frac{dU}{d\rho}\ \exp(i2\pi N_{eq}\rho^2)\,d\rho \qquad (14)$$

where $\rho = \xi/a$ is a normalized radius and N_{eq} is evaluated at $\rho = 1$.

Note that if the illumination $U(\xi)$ has a finite discontinuity, ΔU at any point ρ_o, this will contribute an additional term $-[\exp(ikR)/R]\Delta U \exp(i2\pi N_{eq}\,\rho_o^2)$ to the right hand side of Equation (14). Physically, this additional term just corresponds to the effect of a sharp-edged disc of radius ρ_o and illumination $-\Delta U$, and its contribution to the field $U_D(P)$ can be obtained directly from Equation (12). In particular, if a sharp-edge mirror has an amplitude U_1 at the edge, then $\Delta U(\rho=1) = -U_1$ and this additional term is

14

$$U(P) = [U_1 \exp(ikR/R)] \exp(i2\pi N_{eq}) \quad . \tag{15}$$

It is interesting to note that N_{eq} occurs quite naturally as the phase factor in Equation (14) and periodic behavior would be expected as N_{eq} is varied. More importantly, the integral equation is quite significant in that it provides a semi-quantitative measure of the diffraction perturbation to the resonator mode. If we are to achieve the benefits of a geometrical optics mode, then we should search for the conditions that will cause the integral to go to zero. Equation (14) can be evaluated for arbitrary taper functions (amplitude or phase). It will be shown in the following section how optimum taper functions and their required taper widths can be determined for a resonator configuration.

III. THEORETICAL CALCULATIONS

As shown in the previous section, Equation (14) provides a quantitative measure of the diffractive contribution to the resonator fundamental mode. The fundamental mode profile should most closely resembly the geometrical optics mode for taper widths where this integral reaches a minimum. The fundamental mode loss should, correspondingly, increase toward the geometrical optics value at this point, and then become less lossy as diffraction effects again become important. The losses of the dominant modes have been computed numerically for a number of cases with linear and parabolic tapers of both amplitude and phase and it has been found that the loss follows the expected quasiperiodic behavior. The results of these calculations and a discussion of aperture shaping effects follow below.

A computer code based on the Prony technique described by Siegman and Miller[4] was used to determine the eigenvalues and eigenmodes for all the significant modes. For each eigenmode calculation, spurious modes were eliminated by varying the number of eigenvalues requested and by using

different amplitude vectors in the computations. In all cases, the number of mesh or sample points was at least 15 times the value of N_{eq} so that the modes were accurately described.

Parabolic Reflectivity Taper

Consider now a mirror whose amplitude reflectivity is unity from the center out to $\mu = \rho_o$ and tapers parabolically to zero at the mirror edge. If we assume, as stated earlier, that the amplitude follows the reflectivity dependence, then

$$dU/d\rho = 0 \qquad\qquad \text{for} \quad 0 \leq \rho \leq \rho_o \qquad\qquad (16a)$$

and

$$dU/d\rho = -2 \rho U_o / (1 - \rho_o^2) \quad \text{for} \quad \rho_o < \rho < 1 \; . \qquad (16b)$$

The diffraction contribution obtained from Equation (14) is

$$U_D(P) = \frac{2 U_o \exp(ikR)}{(1 - \rho_o^2)R} \int_{\rho_o}^{1} \exp(i2\pi N_{eq}\, \rho^2) \rho d\rho \; . \qquad (17)$$

After integration,

$$U_D(P) = \frac{U_o \exp[ikR + i\pi N_{eq}(1 + \rho_o^2)]}{R} \cdot \frac{\sin X}{X} \qquad (18)$$

where $X = \pi N_{eq}(1 - \rho_o^2)$.

The single pass losses for all the significant modes of a symmetric, unstable resonator ($N_{eq} = 2.8$) with the parabolically tapered reflectivity

described above are shown in Figure 7. The horizontal scale in this graph denotes the radius at which the taper is initiated and the individual mode losses are read on the vertical scale. The general shape of the loss curve for the fundamental mode (that mode having the least loss) is predicted quite accurately by Equation (18). Notice that the mode loss peaks near the geometrical optics mode loss (75% in this case) each time the diffraction contribution goes to zero. This happens whenever

$$\rho_o = \sqrt{1 - \frac{m}{N_{eq}}} \tag{19}$$

where m is an integer. For N_{eq} = 2.8, the integral becomes zero at ρ_o = 0.802 and ρ_o = 0.535. It is at these points where the mode looks most like the geometrical optics mode, as shown by the parabolic taper mode illustrated in Figure 2. Thus, one can use the simple formulation of Equation (14) to predict an optimum resonator configuration.

It can be seen from Equation (18) and Figure 7 that the effects of the edge taper are very sensitive to the taper region width. To understand this it is useful to think of the tapered region in terms of radial zones, analogous to Fresnel zones, over which the phase term in Equation (18) changes by π. These zones, in addition to aiding the understanding of the integral, are useful as graphical aids to determine the proper width for the tapered region and to estimate the taper shape. This concept of equivalent Fresnel zones is discussed is more detail below in the section on aperture shaping (where it is particularly useful) but can be illustrated here by assuming that the function $dU/\rho d\rho$ varies slowly over the zone widths. This term can then be removed from the integral and Equation (14) can be written in this form:
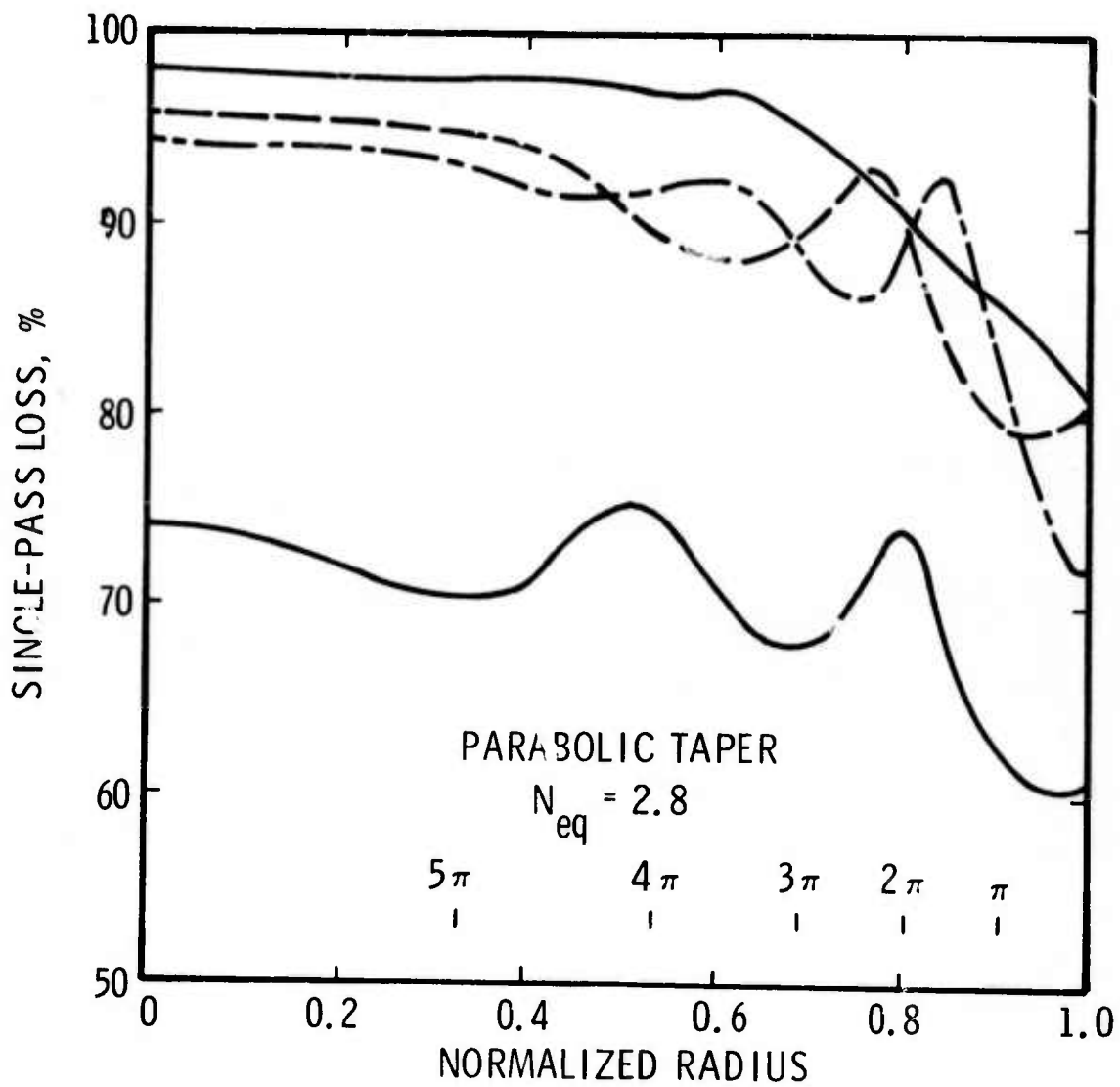
Figure 7.   Single pass loss for the modes of a symmetric unstable resonator with parabolic amplitude reflectivity tapered mirrors as a function of the normalized radius at which the taper begins. $N_{eq} = 2.8$

18

$$U_D(P) \approx \frac{\exp(ikR)}{2R} \cdot \left. \frac{dU}{\rho d\rho} \right|_{\substack{\rho \\ 0}}^{\substack{\rho \\ 0}} \int_{0}^{1} \exp(i2\pi N_{eq} u) du \quad , \tag{20}$$

where $u = \rho^2$.

Two things are apparent from this integral. Firstly, the integral goes to zero when exactly two zones are covered by the tapered region. Secondly, an approximate functional dependence for $dU/d\rho$ is indicated by the require-ment that $dU/\rho d\rho$ vary slowly. Of course, the parabolic dependence described by Equation (16b) satisfies this criterion perfectly in that $dU/\rho d\rho$ is a constant.

A zone is completed each time the phase in Equation (19) changes by π, i.e. each time $N_{eq}(\rho)$ changes by 0.5. The zone radii are marked in Figure 7 by the numbers just above the abcissa indicating each change of π in the phase argument. As the number of zones is increased (as the taper width is increased) then $dU/d\rho$ decreases making the integral value less sensitive to the exact width. Thus, it is generally found that any amount of taper is an improvement over the sharp edge condition but optimum results are expected when the taper region encompasses an even number of zones.

This agrees with Anan'ev's statement that the desired taper width is $a/2N_{eq}$ since for large N_{eq} it can be shown that two zones are covered if the taper extends over this distance. However, this formulation also shows that the modes are alternately improved and degraded as the taper is increased still further.

The discrimination ratio, defined here as the ratio of eigenvalue magnitudes squared, is also sensitive to the type of taper and the taper width. This discrimination ratio, which is a measure of the ability to operate single mode, can be considerably larger than for the sharp edge resonator as

illustrated in Figure 8. In this figure, the ratio of the fundamental to the second symmetric mode is shown and, for some of the tapers, the ratio of the second to the third mode is shown. Crossings of modes as the taper width is varied are apparent, much like Siegman and Miller[4] observed as N_{eq} was varied. For the mode shown in Figure 2 ($\rho_0 = 0.8$), not only are the phase and intensity profiles greatly improved but the discrimination ratio is 2.40 compared to the sharp edge ($\rho_0 = 1$) value of 1.35. The sharp peak in the discrimination ratio near $\rho_0 = 0.8$ suggests that additional minor changes in the mirror reflectivity could result in even higher discrimination ratios.

If the value for N_{eq} is changed, then the zone widths will be changed accordingly. This is illustrated in Figure 9 where the mode losses for $N_{eq} = 3.5$ are shown. In this case there are more zones and the zone widths are, of course, smaller but the general shape of the curves are otherwise the same. As above, the zone radii are marked by the phase values indicated above the abcissa. The narrowing of the zone widths as N_{eq} increases points out that the taper region for large Fresnel number resonators need only perturb a small fraction of the mirror area.

As long as the reflectivity taper function is reasonably smooth, then the phase term in Equation (14) will dominate as described above and the phase zones therefore exist for other taper functions. Although the integral may not go to zero, there will typically be maxima and minima as predicted on the basis of these zones. Linear taper functions have also been studied for several equivalent Fresnel numbers and the results, described below, follow the expected pattern.

Linear Reflectivity Taper

Next, consider a mirror whose amplitude reflectivity is unity from the center to $\rho = \rho_0$ and then tapers linearly to zero at the mirror edge. Then,
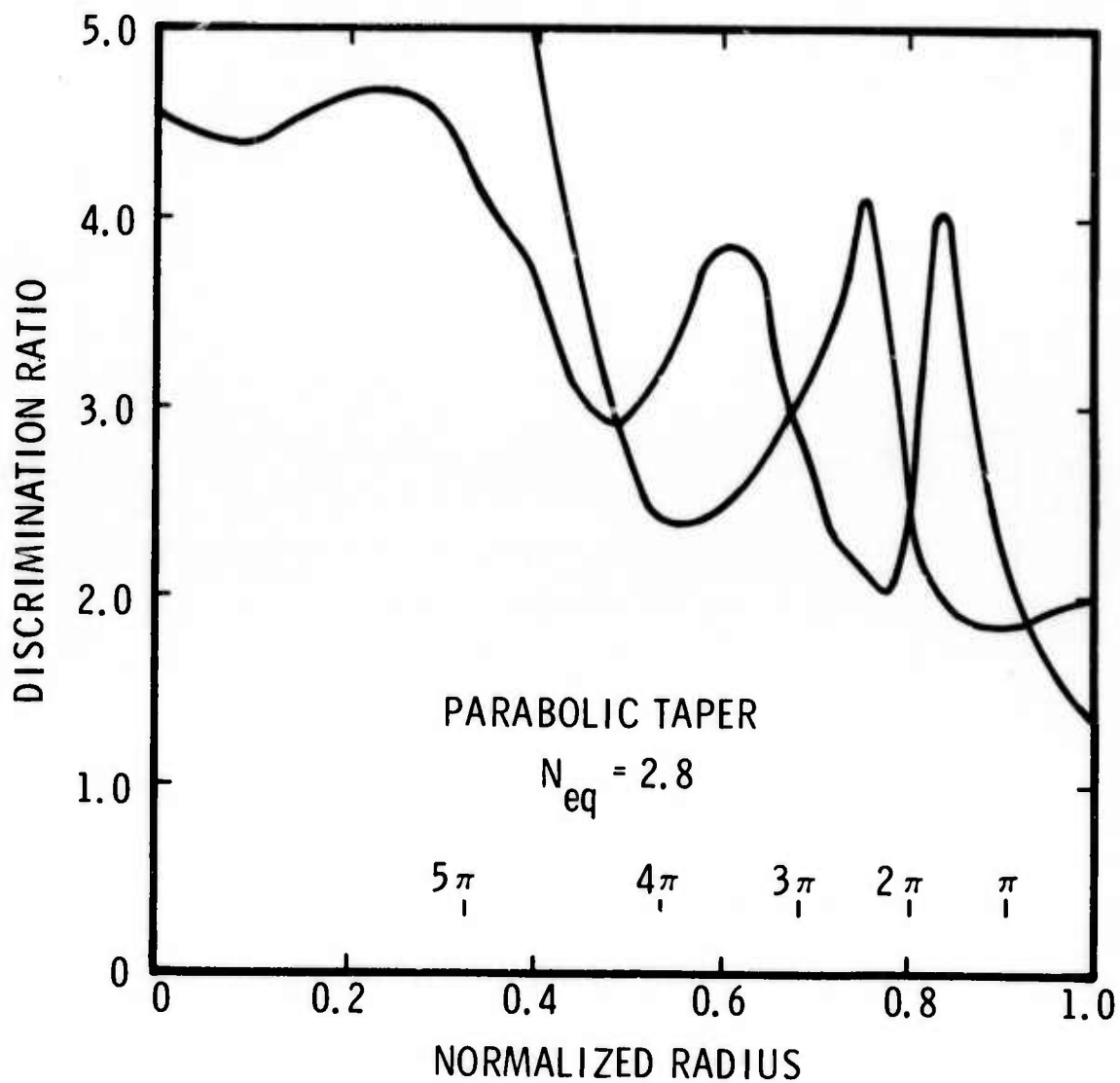
Figure 8.   Mode discrimination ratio for a symmetric unstable
resonator with parabolic amplitude reflectivity
tapered mirrors as a function of the normalized
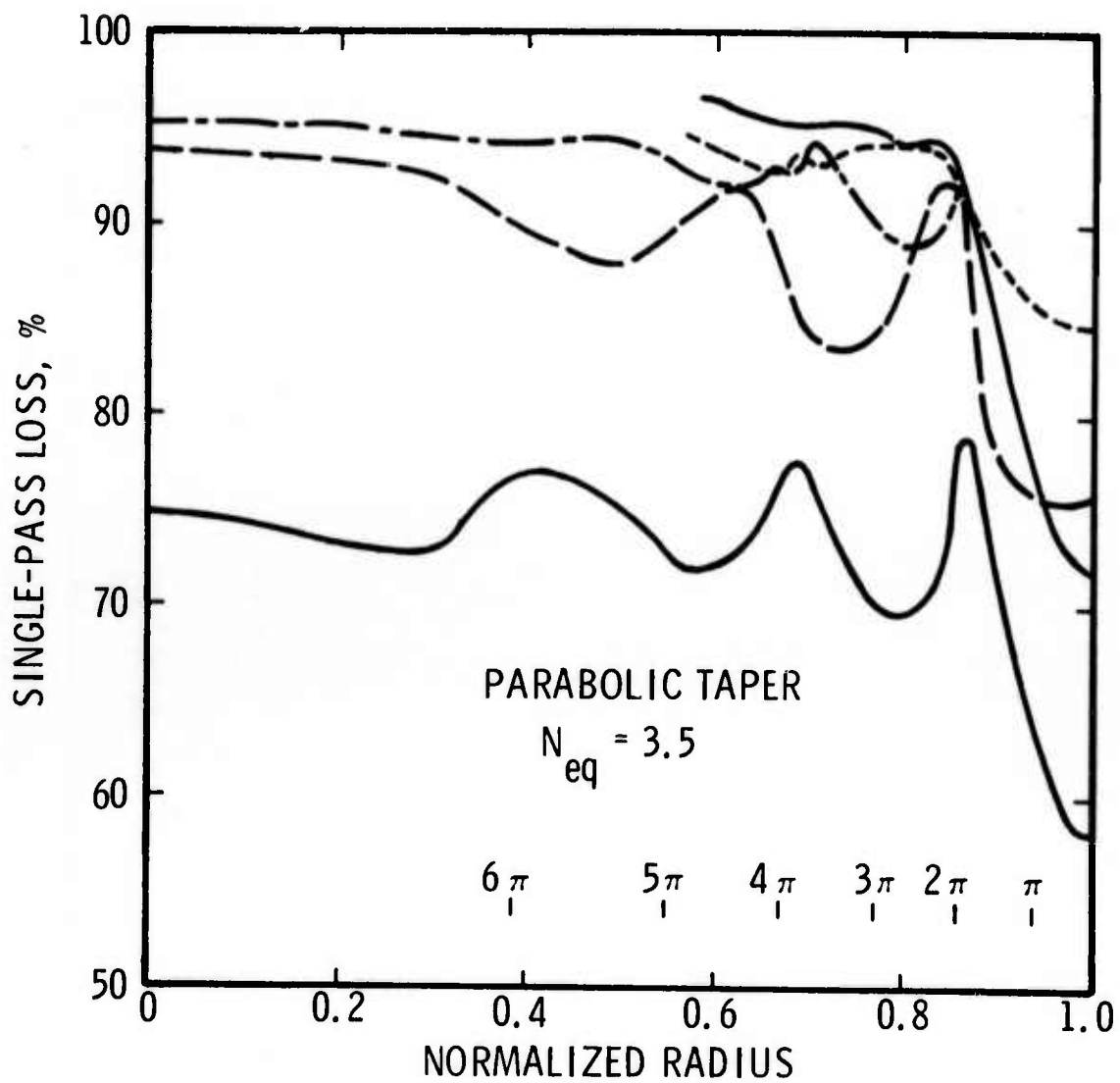radius at which the taper begins. N_{eq} = 2.8

21

Figure 9. Single pass loss for the modes of a symmetric unstable resonator with parabolic amplitude reflectivity tapered mirrors as a function of the normalized radius at which the taper begins. $N_{eq} = 3.5$

$$dU/d\rho = 0 \qquad \text{for} \quad 0 \leq \rho \leq \rho_o \qquad (21a)$$

$$\text{and} \quad dU/d\rho = -U_o/(1-\rho_o) \quad \text{for} \quad \rho_o < \rho < 1 . \qquad (21b)$$

Substituting this into Equation (14) to get the diffraction contribution gives

$$U_D(P) = \frac{U_o \exp(ikR)}{2(1-\rho_o)R\sqrt{N_{eq}}} \int_{\rho_o 2\sqrt{N_{eq}}}^{2\sqrt{N_{eq}}} \exp(i\pi v^2/2)\, dv \qquad (22)$$

where $v = 2\sqrt{N_{eq}}\, \rho$. This integral has the form of the Fresnel integrals[7] which define the coordinates on a Cornu spiral and which have tabulated values. When v is approximately 1.5 or larger, then the phase variation becomes the dominant factor and the integral resembles a vibration spiral. The results are then predictable on the basis of the zones described above for the parabolic taper. Although the integral does not go to zero, it reaches a minimum each time the tapered region encompasses an even number of zones. The mode losses for a symmetric, unstable resonator with $N_{eq} = 2.8$ are illustrated in Figure 10 and show the expected periodic behavior. Notice that the fundamental mode loss does not reach the geometrical optics mode loss (75% again in this case) as it did for the parabolic taper and the mode shape at the first loss peak ($\rho_o \approx 0.8$), shown in Figure 2, is not as desirable as the parabolic taper. Thus, just as evaluation of Equation (22) suggests, the linear taper can effect a considerable improvement over the sharp edge resonator but does not reach the optimum condition.

For high power lasers, introducing a reflectivity taper is not simple and may not be practical because of damage to the mirrors or attenuating apertures. Similar effects can be accomplished by making the mirrors slightly aspheric, thereby introducing a phase taper. This may be more practical from a construction standpoint and is discussed below.
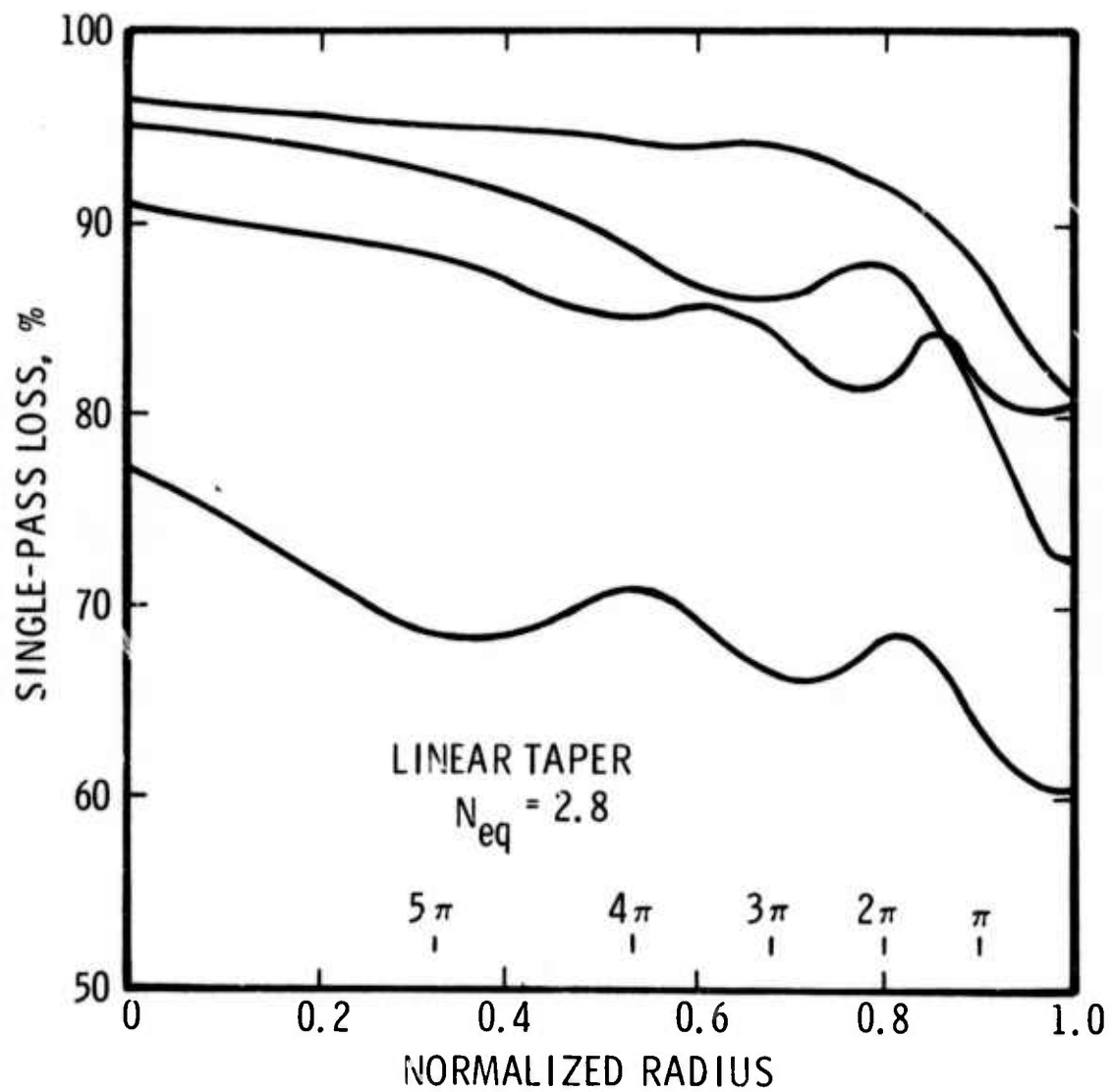
Figure 10. Single pass loss for a symmetric unstable resonator with linear reflectivity tapered mirrors as a function of the normalized radius at which the taper begins. $N_{eq} = 2.8$

24

Parabolic Phase Taper

Consider now mirrors whose edges have been gound off so that over a portion of the mirror, the phase of the reflected wave differs from the geometrical spherical wave. In particular consider a mirror where this deviation from spherical varies parabolically with the aperture radius. The phase difference from the geometrical wave is given by

$$\phi = -\phi_o \qquad \text{for} \quad 0 \le \rho \le \rho_o \qquad (23a)$$

$$\phi = -\phi_o \frac{(\rho^2 - 1)}{(\rho_o^2 - 1)} \qquad \text{for} \quad \rho_o \le \rho \le 1 \qquad (23b)$$

so that

$$U(\rho) = U_o \exp[-i \phi_o (\rho^2 - 1)/(\rho_o^2 - 1)] \qquad (24)$$

where ϕ_o is the magnitude of the total taper. Note that in our notation, if ϕ_o is positive, the mirror edges have been ground off by $\phi_o/2k$, or, alternately the center has been built up by this amount. Then,

$$dU/d\rho = 0 \qquad \text{for} \quad 0 \le \rho \le \rho_o \qquad (25a)$$

and

$$dU/d\rho = \frac{-i2\rho \phi_o U_o}{(\rho_o^2 - 1)} \qquad \text{for} \quad \rho_o \le \rho \le 1 \ . \qquad (25b)$$

Substitution into Equation (14) gives the diffraction contribution

$$U_D(P) = \frac{U_o \exp(ikR)}{R} \left\{ \int_{\rho_o}^{1} \frac{2i\,\phi_o}{(\rho_o^2 - 1)} \cdot \exp\left[-i\,\phi_o\left(\frac{\rho^2 - 1}{\rho_o^2 - 1}\right) + i2\pi N_{eq}\,\rho^2 \right] \rho d\rho \right.$$

$$\left. + \exp\left(i2\pi N_{eq}\right) \right\} \quad . \tag{26}$$

After integration and rearranging terms this becomes

$$U_D(P) = \frac{U_o \exp(ikR + i2\pi N_{eq})}{R} \left\{ \frac{\phi_o}{\phi_1}\,[1 - \exp(i\,\phi_1)] + 1 \right\} \tag{27}$$

where

$$\phi_1 = 2\pi N_{eq}\,(\rho_o^2 - 1) - \phi_o \tag{28}$$

To make the diffracted field zero will require that $\phi_1 = -(2n+1)\pi$ where n is an integer and $\phi_o = -\phi_1/2$. This requires that

$$\phi_o = (n + 1/2)\pi \tag{29}$$

$$\rho_o^2 = 1 - \frac{n + 1/2}{2N_{eq}} \quad . \tag{30}$$

These expressions give the amount of phase roll off and the radius at which the taper begins. Notice that the negative ϕ_o solution are not possible since that requires $\rho_o > 1$, hence the diffracted field can be made zero only for mirrors whose edges have been ground off and not for mirrors whose edges have been built up. For a given N_{eq} there is a finite number of sets of values for ϕ_o and ρ_o.

To check these conclusions the eigenvalues were calculated on the computer for the case $\phi_0 = +\pi/2$, $N_{eq} = 2.8$, and $M = 2$. The single pass losses for the first three modes are shown in Figure 11. The values of the parameter ϕ_1 are also shown on the figure. The computer results closely follow the theoretical predictions and again demonstrate the validity of the theory. For this case, the diffracted field at P is zero when $\rho_0 \approx 0.96(\phi_0 = -\pi)$ and the computer results show a sharp loss peak at this point with the single pass losses approaching the geometrical loss value of 75%.

The other features of the loss curve such as the rapid variation near $\phi_1 = -\pi$ and the slow undulations elsewhere are also consistant with the theory. The phase taper, in contrast to the amplitude taper, has the added term [see Equation (26)] resulting from the sharp edge which is still present. Because of this term only one null is reached and, for other taper widths, minima and maxima occur but the excursion is very small. Thus, the behavior patterns for phase tapers is different from that for amplitude tapers but the improvements that can be effected are the same.

Aperture Shaping

Consider now a totally reflecting, spherical mirror which is noncircular but which is uniformly illuminated by a spherical wave emanating from the virtual focus. The diffraction contribution at the opposite virtual focus can be obtained from Equation (12) and if the boundary path Γ is chosen properly, this contribution will go to zero or at least reach a minimum. Thus, it is possible to realize the same benefits as in the case of amplitude or phase tapering by simply choosing the appropriate mirror boundary shape. Generation of an optimum boundary shape will be discussed first, followed by a discussion of the more common mirror shapes, including circles, squares and rectangles.
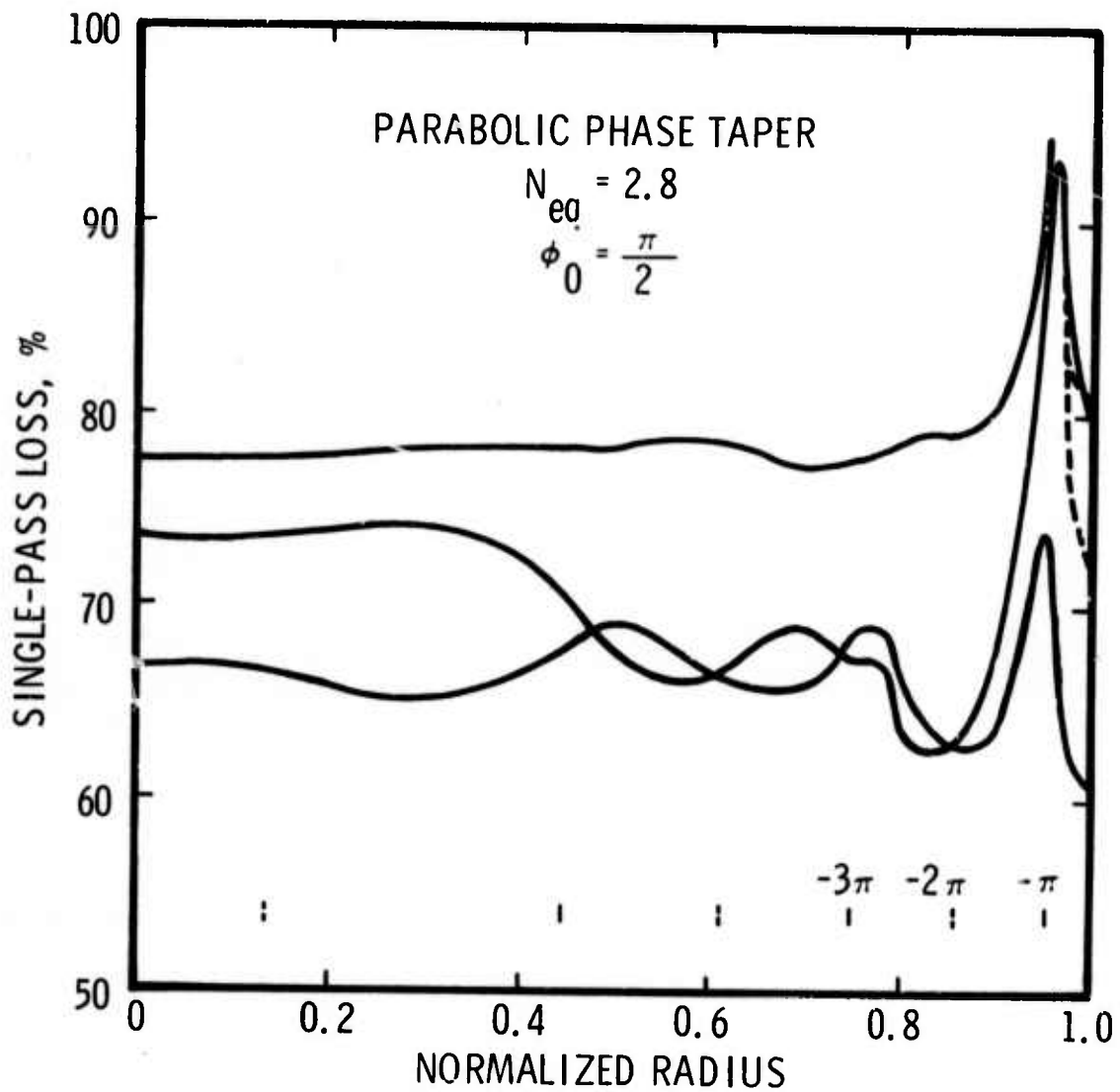
Figure 11. Single pass loss for a symmetric unstable resonator with parabolic phase tapered mirrors as a function of the normalized radius at which the taper begins. $N_{eq} = 2.8$

It is apparent from Equation (12) that if we have a mirror shape such that

$$dl = \frac{\xi^2}{a} \, d\xi \tag{31}$$

where a is the minimum radius, then

$$U_D(P) = \frac{-U_o \exp(ikR)}{R} \int_1^{\rho_M} \exp(i2\pi N_{eq} \rho^2) \rho \, d\rho \tag{32}$$

where $\rho = \xi/a$ and $N_{eq} = N_{eq}(a)$. If the minimum ($\rho = 1$) and the maximum ($\rho = \rho_M$) radii are chosen so that $N_{eq}(\rho_M^2 - 1)$ is an integer then the diffraction contribution goes to zero and the mode should be nearly optimum. The path taken in going from $\rho = 1$ to ρ_M, which is the boundary shape, can be found in the normalized cylindrical coordinates (ρ, θ) from Equation (31)

$$\frac{dl}{a} = \sqrt{d\rho^2 + \rho^2 \, d\theta^2} = \rho^2 \, d\rho \tag{33}$$

which therefore requires that

$$\frac{\sqrt{\rho^4 - 1}}{\rho} \frac{d\rho}{} = d\theta \quad . \tag{34}$$

Integrating both sides of the equation results in a transcendental equation in ρ and θ,

$$\cos\left(2\theta - \sqrt{\rho^4 - 1}\right) = 1/\rho^2 \quad . \tag{35}$$

The solid curve plotted in Figure 12 for $0 \leq \theta \leq \pi/4$ is a solution to this equation with the normalization that the minimum radius ($\rho = 1$) occurs at $\theta = 0$.

An ideal mirror boundary shape can be produced by using any combination of segments of the curve given by Equation (35) and hence there are any number of solutions such as the two illustrated in Figure 12. It is only necessary that (1) each segment cover the proper width for the integral in Equation (32) to contribute zero over the segment, and (2) each segment must cover an angle of π/n radians (n = integer) so the required symmetry will be achieved.

The first requirement above is just the requirement that the segment cover an even number of equivalent Fresnel zones. That is, the phase argument $(2\pi N_{eq} \rho^2)$ in Equation (32) must change by $m2\pi$ where m is an integer or, equivalently, $N_{eq}(\rho)$ must change by an integer over the segment. The solid curve of Figure 12 is therefore one quadrant of a perfect aperture shape with n = 4 and N_{eq} changes by three on each segment. The dashed curve is another perfect aperture shape with n = 4 and N_{eq} changes by one on each segment.

The above example is an illustration of how equivalent Fresnel zones can be used for graphically determining the width of the region over which the mirror boundary should be altered and the approximate shape the boundary should take. For mirrors whose radius varies slowly with angle (e.g., mirrors which are approximately circular), $\int dl/\xi$ can be considered constant over one zone and the changes in aperture shape should cover an even number of zones, i.e. the difference between the minimum and maximum radii should be an even number of zones. The correctness of the phase generated can be estimated by comparing it with any segment of the optimum
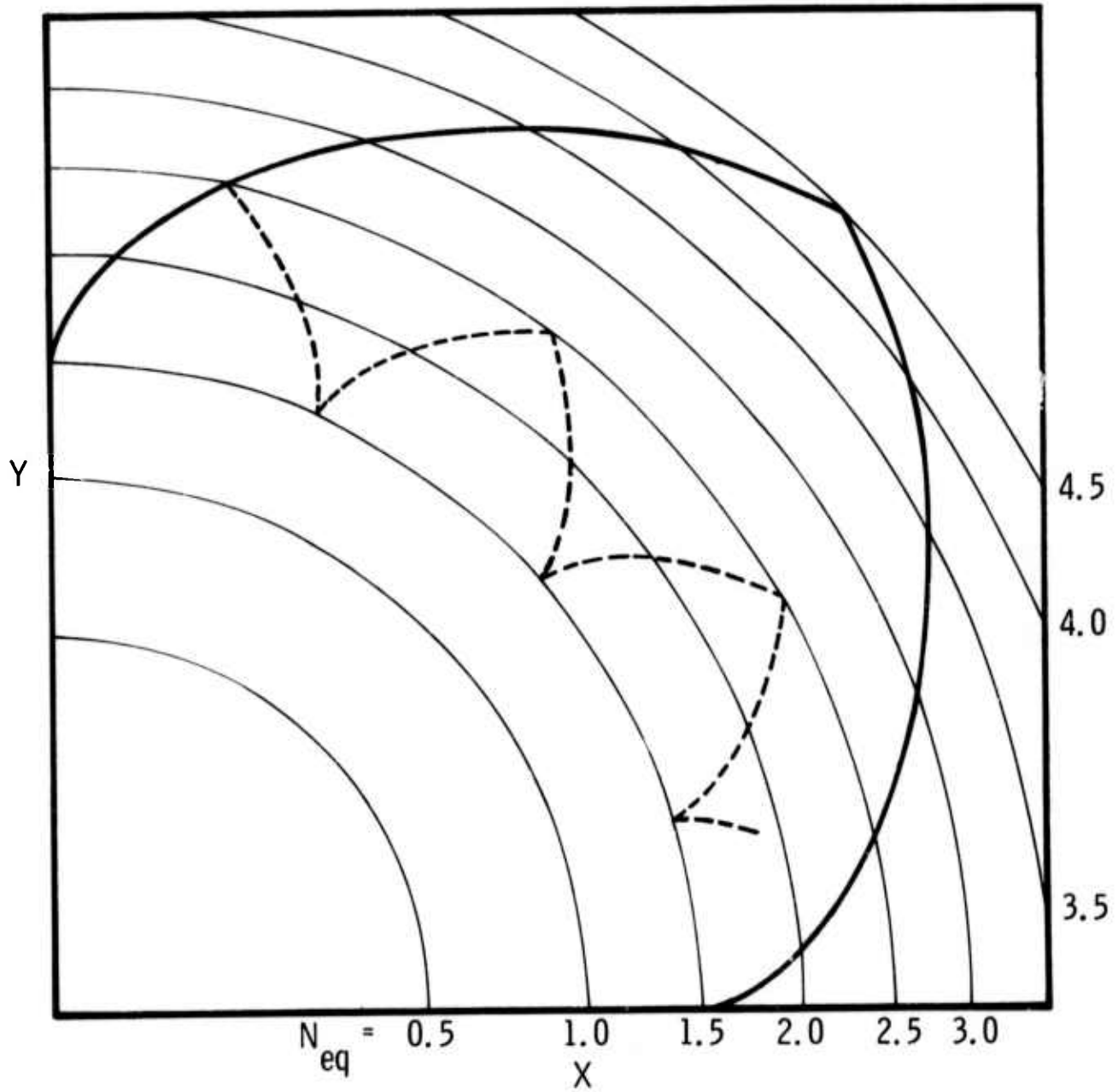
Figure 12. Two examples of optimum aperture shapes to reduce edge diffraction effects.

curve given by Equation (35). For example, consider an elliptical mirror with a maximum radius such that the maximum $N_{eq}(\rho) = 7.0$. One choice for a minimum $N_{eq}(\rho)$ is 5.0 (4 zones crossed) and this is illustrated by the solid curve in Figure 13.

The extent to which the ellipse (or any curve) nulls the diffracted field can be estimated by comparison with the optimum curve given by Equation (35). For comparison to the ellipse, the boundary conditions on this equation require at the curve coincide with the ellipse at two points separated by an angle $\Delta\theta = \pi/2$. This is illustrated in Figure 13 (where the two curves coincide at $\theta = \pi$ and $\theta = 3\pi/2$) and it is apparent that the third quadrant of the ellipse, which repeats in each of the other quadrants, does not differ greatly from the optimum shape given by the dotted line. Preliminary experiments have shown that an elliptical boundary shape similar to the shape shown in Figure 13 does result in an improved resonator mode profile.

The zone concept is also useful for graphically estimating the behavior of more common mirror shapes. The most common, the circle, is also the worst shape as far as diffractive effects are concerned. All of the diffractive contributions from the edge add up in phase at the virtual focus and result in a contribution $U(P) = U_o \exp(ikR + 2\pi N_{eq})/R$ as described in Equation (15). This results in mode patterns with large phase and amplitude ripples as shown in Figures 2 and 3.

It may be that beneficial cancellation effects introduced by slight angular misalignment of a circular mirror may outweigh the undesirable asymmetry caused by the misalignment. Equivalent Fresnel zones can also be used to analyze misaligned resonators. In this case the center of the Fresnel zones does not correspond to the mirror center. The
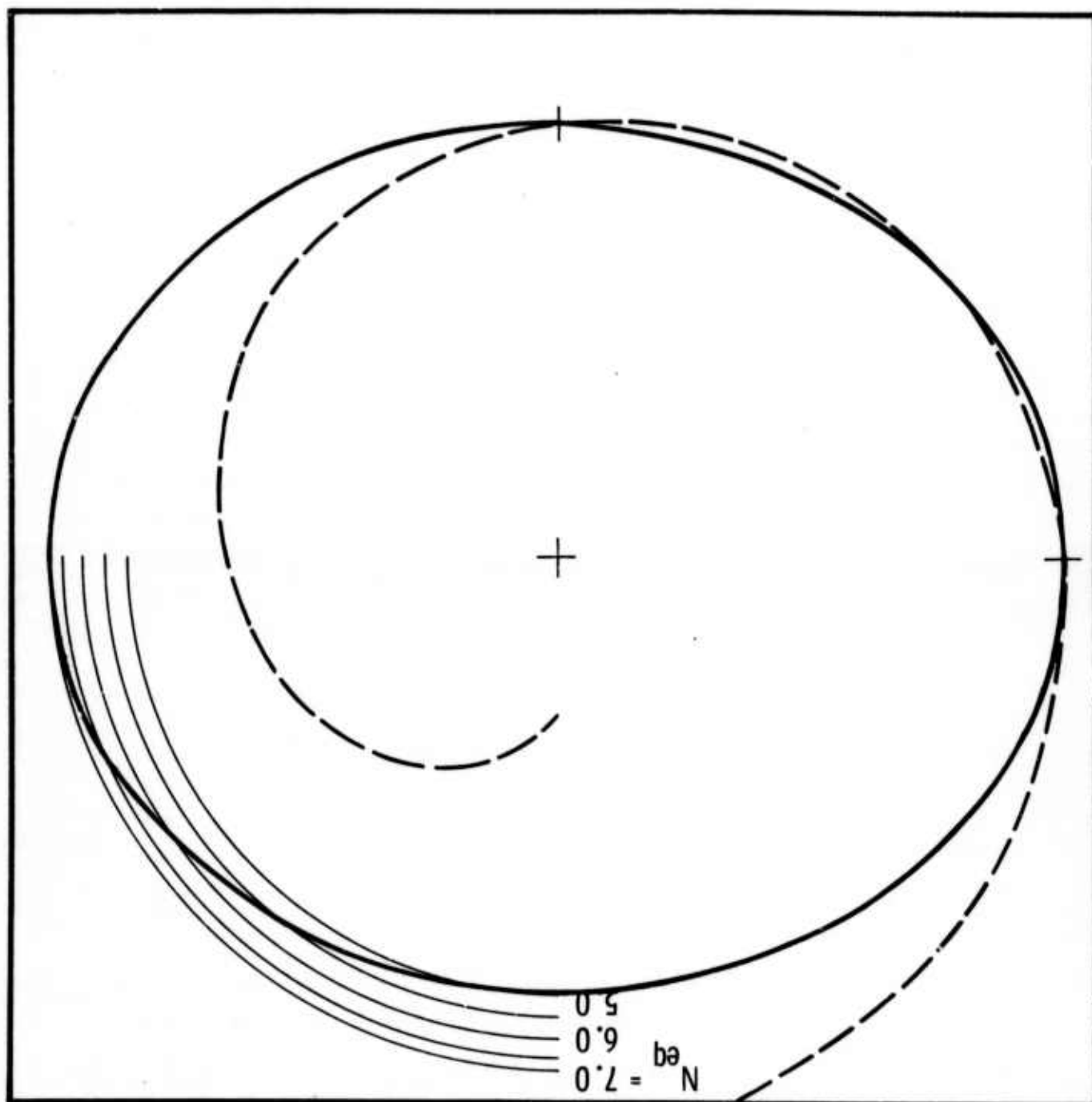
Figure 13. The elliptical shaped aperture covering four zones compared to the optimum aperture shape.

edge diffraction field can be estimated from the phases of the zones
through which the mirror boundary passes and the boundary length in
each zone.

It is expected that a square mirror with a reasonably large equivalent
Fresnel number will be inherently better than a circular mirror because
the boundary crosses several zones and partial cancellation of the
diffraction contribution occurs. Graphically this is illustrated in
Figure 14 where a square mirror boundary with N_{eq} ($\rho = \sqrt{2}$) = 4 is
plotted. Starting at the corner, as the boundary is traversed, alternate
zones (π out of phase) are crossed leading to partial cancellation. It can
be seen, however, that the segment length in the smallest radius zone
tends to be much larger than the others and complete cancellation is
difficult, if not impossible. Based on this picture, it is expected that
the square mirror would give better results than a circular mirror but
would not be optimum. To show this, the diffractive contribution for a
square aperture of side 2a can be computed from Equation (12) as:

$$U_D(P) = \frac{-U_o \, \exp(ikR + i2\pi N_{eq})}{\pi R \sqrt{N_{eq}}} \int_{-2\sqrt{N_{eq}}}^{+2\sqrt{N_{eq}}} \frac{\exp(i\pi v^2/2)}{\sqrt{\dfrac{v^2}{4N_{eq}} + 1}} \, dv \qquad (36)$$

where (x, y) are the rectangular coordinates, $v = 2\sqrt{N_{eq}} \, x/a$ and
$N_{eq} = N_{eq}(a)$. The form of this integral is similar to that producing a
Cornu spiral and the large contribution near the minimum value of v
(the region of the smallest radius zone) will never be cancelled just as
a Cornu spiral curve never returns to the origin. This situation can be
corrected by modifying the straight line boundary so that it resembles the
optimum curve of Figure 12 in the smallest radius zone or by making the
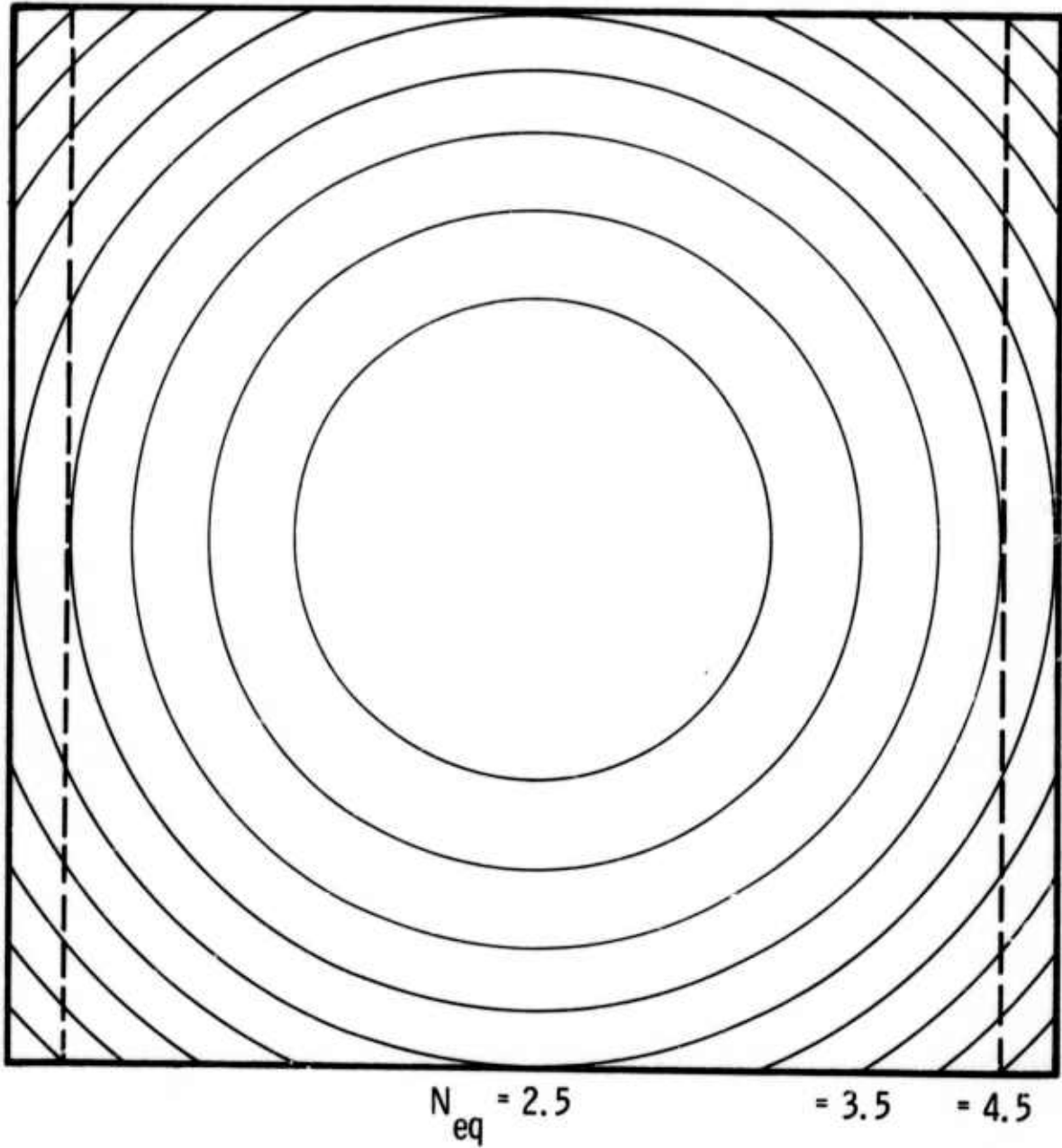mirror slightly rectangular. As is shown by the dotted boundary in

Figure 14. The square and rectangular shaped apertures with equivalent Fresnel zones.

Figure 14, when two opposite sides are reduced by one equivalent
Fresnel zone then the long segment length (which occur in the smallest
zones) on adjacent sides of the rectangle are out of phase and tend to
cancel. This would then be expected to result in an improvement over
the square profile.

IV. CONCLUSIONS

The results presented here show that significant improvements in the
amplitude and phase of the dominant mode and increases in the mode
discrimination ration are attainable by mirror tapering or aperture
shaping. The simple theory developed here for the diffractive contri-
bution to the resonator fields can be used to design optimum resonators
without resorting to extensive machine calculations. Using these results,
it should be possible to design unstable cavities which have reduced
internal hot spots and outputs which are more nearly diffraction limited.
We have not included in this work any effects of gain medium nonuniformity.

The equivalent Fresnel zone concept, developed in Section III, is useful
in the design of resonators and in gaining physical insight into the mode
phenomena. In particular, the physical significance of N_{eq} as a phase
factor is clear from the discussions in the text. It should be pointed out
that, with the exception of a factor of two occuring in the definition of
N_{eq}, the equivalent Fresnel number is just the Fresnel number based on
a curved wavefront. One can use these concepts to predict and understand
unstable mode patterns even in sharp edge cases. These concepts will be
expanded upon in a forthcoming publication where they are related to
experimental observations.

It is also clear from these results that for large Fresnel number systems
the mode obtained in practice may be quite different from those predicted

36

by the sharp edge theory. Small discontinuities in the edge can easily cover two or more equivalent Fresnel zones when the Fresnel number is large and hence the amplitude of the diffraction fields can be significantly changed. In fact, for very large equivalent Fresnel numbers the outer zone widths become so small that these perturbations may be unavoidable resulting in inherently better (although not necessarily optimum) mode quality.

REFERENCES

1. A. E. Siegman, "Unstable Optical Resonators for Laser Applications," Proc. IEEE 53, 277-287 (March 1965).

    Also see:

    W. Streifer, "Modes in Unstable Optical Resonators," IEEE J. Quant. Elect. QE-4, 229 (April 1968)

    Also see:

    D. B. Rensch and A. N. Chester, "Interactive Diffraction Calculations of Transverse Mode Distributions in Confocal Unstable Laser Resonators," Appl. Opt. 12, 997 (May 1973).

2. H. Kogelnik and T. Li, "Laser Beams and Resonators," Proc. IEEE 54, 1312 (October 1966), and Appl. Opt. 5, 1550 (October 1966).

3. A. E. Siegman and R. W. Arrathoon, "Modes in Unstable Optical Resonators and Lens Waveguides," IEEE J. Quant. Elect. QE-3, 156 (April 1967).

4. A. E. Siegman and H. Y. Miller, "Unstable Optical Resonator Loss Calculations Using the Prony Method," Appl. Opt. 9, 2729-2736 (December 1970).

5. Yu. A. Anan'ev, "Unstable Resonators and Their Applications (Review)," Sov. J. Quant. Elect. 1, 565 (May/June 1972).

    Also see:

    Yu. A. Anan'ev and V. E. Sherstobitov, "Influence of the Edge Effects on the Properties of Unstable Resonators," Sov. J. Quant. Elect. 1, 263 (November/December 1971).

6. H. Zucker, "Optical Resonators with Variable Reflectivity Mirrirs," Bell Sys. Tech. J. 49, 2349-2376 (November 1970).

7. M. Born and E. Wolf, Principles of Optics, The MacMillian Company, New York, New York (1964).